THE JOURNAL OF PHYSICAL CHEMISTRY C

C: Surfaces, Interfaces, Porous Materials, and Catalysis

Fluid Property Affected Splashing in Teapot Effect

Lichun Shi, Yuanzhe Li, Yonggang Meng, Guoqing Hu, and Yu Tian

J. Phys. Chem. C, **Just Accepted Manuscript** • DOI: 10.1021/acs.jpcc.8b05613 • Publication Date (Web): 27 Aug 2018

ACS Publications

is published by the American Chemical Society. 1155 Sixteenth Street N.W., Washington, DC 20036

Fluid Property Affected Splashing in Teapot Effect

Lichun Shi, † Yuanzhe Li, † Yonggang Meng,† Guoqing Hu‡§,Yu Tian†*

†State Key Laboratory of Tribology, Tsinghua University, Beijing 100084, China

‡ State Key Laboratory of Nonlinear Mechanics, Institute of Mechanics, Chinese Academy of Sciences, Beijing 100190, China

§ School of Engineering Science, University of Chinese Academy of Sciences, Beijing 100049, China

ABSTRACT

Liquid flowing on a curved solid surface usually leads to a typical teapot effect. As the increase of jet velocity, the liquid could detach from a curved solid surface completely in one streamline or partially in multiple streamlines. The latter we called splashing. Former studies attributed the splashing behavior to the breaking of the balance between the centrifugal force and the pressure drop across the liquid flow. This study disclosed that the parameters of surface tension, viscosity and additive molecules of liquid significantly affected the jet splashing in teapot effect. A liquid with higher Weber number (lower surface tension) and lower Reynolds number (higher viscosity) prefers to separate from the solid surface in one streamline. Besides, liquid with larger molecular weight additives is easier to splash. Molecular dynamics simulations disclosed that higher water molecule density around the additive molecules with larger cohesive force could more effectively

suppress splashing. There is no splashing when the cohesive force is larger than the capillary adhesion force. Otherwise splashing would occur. This study discloses the importance of cohesive force in the splashing in teapot effect, which might provide an effective guide for industrial applications to tuning the splashing.

1. INTRODUCTION

When tea water is slowly poured out from a teapot, it often flows downwards to the bottom surface of the spout, instead of falling into the cup. Only when the flow velocity increases to large enough values, the tea water could be poured into a cup. This phenomenon is generally called "teapot effect". The flow behaviors in teapot effect vary with the flow velocity. When increasing the flow velocity, the fluid would separate from the solid surface in a single streamline or splash into several streamlines. This effect involves hydrodynamic process of liquid jet and wetting property of the solid surface. The teapot effect is closely related to aircraft design,[1] raindrop effect on flying insects,[2] heart disease diagnosis,[3] fire safety[4] and mechanical lubrication.[5,6]

Most researches focused on the overflow and separation behaviors in teapot effect. When the teapot effect was firstly studied about 60 years ago, Marcus Reiner experimentally showed that the overflow is not due to the surface tension or the adhesion of liquid to solid surface.[7] It was theoretically explained as a purely hydrodynamic process by Keller. The pressure in the curved flow increases as the increase of distance from the center of the streamline curvature to the flow surface, and the pressure difference between the outer surface and the inner surface of flow would make the liquid jet show attracted by the solid surface.[8,9] Vanden-Broeck and Keller considered the gravity effect based this similar hydrodynamic theory.[10,11]

However, recent studies have proved that the pressure drop in liquid jet due to the bending of liquid streamline, which is classically described as the Coanda effect,[12-14] is not the only reason for the overflow behavior in teapot effect. Duez et al studied the flow ejection angle from the curved solid with different surface wettability. They showed that when the surface was superhydrophobic, the liquid jet was hard to overflow on the solid surface. [15] Considering the balance between the centrifugal force and the hydro-capillary adhesion force, Duez et al predicted that the deviation angle of liquid jet increased as the increase of contact angle, and the separation velocity was linearly proportional to the radius of curved surface.[16] Dong et al studied the overflow behavior on solid surfaces with different wettability and radius. They concluded that the separation velocity was dependent on the quadratic root of the curved solid radius.[17] Bouwhuis et al indicated the same conclusions with Dong's experiment results by theoretical analysis. [18,19] Kibar studied liquid jet impingement on a convex surface with different wettability. The liquid jet could be reflected off the superhydrophobic convex surface no matter how slow the velocity was, and the reflection angle was independent on the curvature of solid surface. He concluded that the capillary adhesion force between the solid surface and liquid determined the liquid jet separation behavior. [20,21]

In most studies on teapot effect, the liquid viscosity effect on separation behavior was considered unimportant and supposed to be negligible. [22,23] However, Isshiki et al built a theoretical model for a sheet flow on a circular cylinder considering the energy dissipation induced by the viscous friction and neglected the surface tension effect. They thought that when the average velocity in the theoretical model equaled zero, the liquid would separate from the circular cylinder surface. The results showed the importance of viscosity in the separation behavior of teapot effect,[24] which was contradictory with the previous studies.[16] This contradictory implies that the fluid property part of the teapot effect deserves further clarification.

Up to now, few researches about the teapot effect have been focused on the mechanism of splashing behaviors (partial separation with several streamlines). The reason for splashing behavior is usually explained that the centrifugal force exceeds the pressure drop across the flow. However, the maximum pressure difference across the flow could be as large as the external atmospheric pressure, which is estimated three orders of magnitude larger than the centrifugal force for the system in this work. In this condition, the splash or separation would never occur. This means that the pressure drop is not the key factor to affect the splashing. From the view of intermolecular interaction, the flow splashing behaviors mainly result from the breaking of the balance between the centrifugal force and the “cohesive force”, which is generated between the flow sheets when trying to separate them. Combined with the former research that the flow separation behaviors mainly resulted from the breaking of the balance between the centrifugal force and the capillary adhesion force, [15-20] it can be concluded that the relative magnitude of the cohesive force and capillary adhesion force significantly affects the flow patterns evolving from overflow into splashing or separation, under the effect of centrifugal force.

In this work, the effects of liquid property such as surface tension, viscosity and additives on the splashing behaviors in teapot effect were studied. Cohesive force between the flow sheets was found to be one of the most important factors in splashing behaviors. To reveal the roles of liquid viscosity and additives on affecting the cohesive force, a finite element simulation model and a molecular dynamics simulation model were built. The results indicate that the cohesive force is closely related to the number density and location of water molecules near the additive molecules.

2. EXPERIMENTAL METHOD

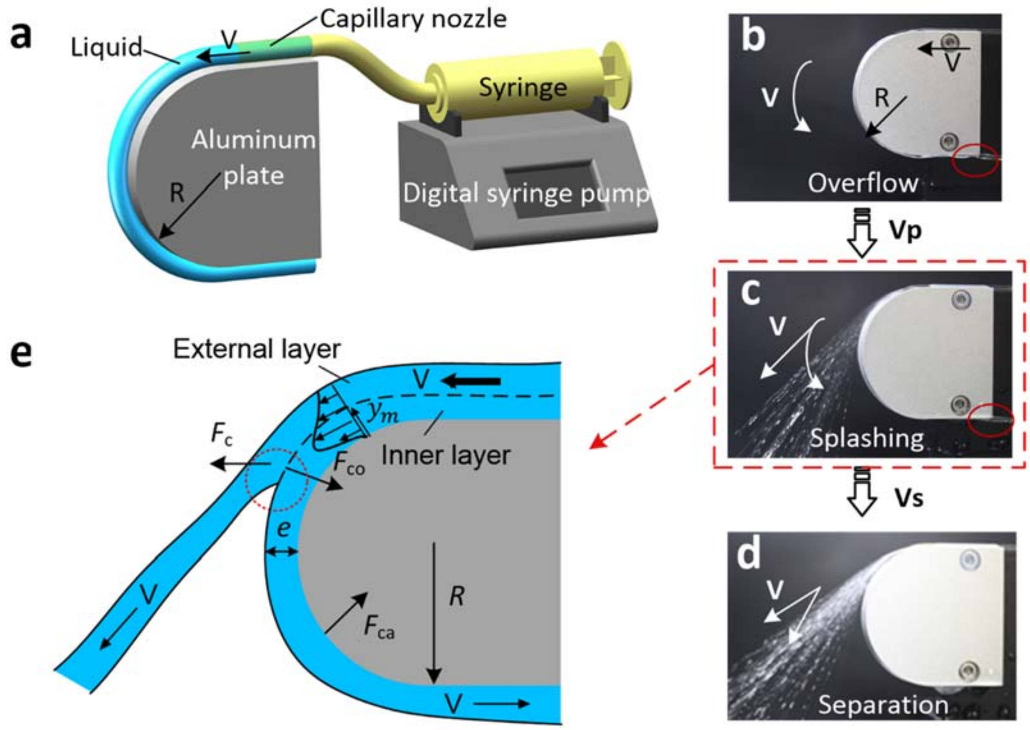

Figure 1. Schematic of the experiment. (a) Schematic of the test system. The flow was drove by a digital syringe pump (RISTRON, RSP02-B, Zhejiang, China) and the nozzle was a capillary tube with an inner diameter of 1 mm. The radius of aluminum plates, *R*, ranged from 5 mm to 40 mm. (b)(c)(d) Flow behaviors evolve with the increase of average outflow velocity. For water solution, the flow behaviors will present overflow (b), splashing (c) and separation (d) successively. (e) Schematic of splashing behavior. F_c, F_{ca} and F_{co} represent the centrifugal force, capillary adhesion force and cohesive force between the stream layers, respectively.

In this study, the experimental apparatus used to study the teapot effect is shown in Figure 1a. The distilled water was added with sodium dodecyl sulfate (SDS), glycerin (GL), polyethylene glycol (PEG) and polyacrylamide (PAM) to change the liquid surface tension, viscosity and additives. The property of the solutions is shown in Table 1.

The average velocity of liquid flow varied from 1 to 4 m/s, which was changed by setting different flux of the digital syringe pump. The average flow velocity is estimated from:

$$v \approx Q/\pi r^2 \qquad (1),$$

where Q is the flux of the digital syringe pump, r is the inner radius of the capillary nozzle. As the flow velocity increased, the flow behaviors can be divided into three distinct patterns according to the flow separation conditions: overflow (Figure 1b), splashing (Figure 1c) and separation (Figure 1d). More images of the evolution of flow behaviors with the flow velocities and curved surface radius are shown in Figure S1(SI Section S1). The critical velocity that the flow pattern turns from overflow into splashing is defined as V_p (denoted as splashing velocity). The critical velocity that the flow pattern turns from splashing into complete separation is defined as V_s (denoted as separation velocity). In our experiment, the tests to get V_s and V_p are repeated at least three times. And the difference between V_s and V_p is defined as V_d (denoted as difference velocity) to characterize the splashing behavior. It takes the form

$$V_d = V_s - V_p \qquad (2).$$

Table 1. Property of solutions used in the experiment.

No.	Liquid	Viscosity η (mPa · s)	Surface Tension γ (mN/m)	Contact angle θ (°)	Molecular Weight M (g/mol)	Density ρ (kg/m^3)
1	water	1.0	72.9	73.2	18	1,000
2	SDS-5 mM	1.0	42.2	57.7	288.38	1,000
3	SDS-10 mM	1.0	35.1	47.8	288.38	1,000
4	SDS-30 mM	1.0	35.1	44.6	288.38	1,000
5	GL-10%	1.2	71.6	72.8	92.09	1,048
6	GL-25%	1.6	68.2	76.3	92.09	1,075
7	GL-40%	3.1	66.3	78.2	92.09	1,125

8	PEG-2%	1.3	48.6	61.9	20,000	1,012
9	PEG-10%	3.4	42.2	74.5	20,000	1,036
10	PAM-1‰	--	70.3	71.4	5 million	1,000
11	PAM-2‰	--	69.8	74.5	5 million	1,007

Note: All values were given at room temperature. A rheometer (Anton Paar, MCR302) and an electronic balance (ME235S, Sartorius Corp) were used to measure the liquids viscosity and density, respectively. The liquid surface tension was got by a surface tension meter (dataphysics, DCAT21). The contact angle of the liquids on an aluminum plate were got by a contact angle meter (dataphysics, OCA25) with the syringe tip diameter of 0.51 mm. The viscosity of PAM solution is shown in Figure S3a.

3. SIMULATION METHOD

Numerical simulation is an effective method to study fluid behaviors such as the teapot effect.[25,26] A two-dimensional finite element simulation model was built based on COMSOL Multiphysics software (COMSOL Inc.) and a level set method [27,28] was used to calculate the velocity contour (shown in Figure S2a). The inlet boundary is set as the flow rate condition and the wetted wall is the aluminum plate. Different viscosity solutions were simulated with the same inlet flow velocity (e.g. 2.5m/s) to disclose their velocity contours. In this case, the Reynold number of the inlet flow of water and 40%-glycerin are approximate 2500 and 908, respectively.

To clarify the role of additive solutes in the flow splashing behavior, a molecular dynamics simulation model (shown in Figure S2b) was built based on the Forcite module in the Materials Studio software (Accelrys Inc.) to calculate the bonding energy between water and additive molecules[29,30]. A typical cell containing 8630 atoms is composed of 10 additive molecules and 2000 water molecules. The potential energy of molecules is derived from the COMPASS force field in the NPT ensemble. The cut off distance for van der Waals and electrostatic forces is

18.50 Å. More details about the simulations are presented in the section S2 of Supporting Information (SI Section S2).

4. RESULTS AND DISCUSSION

When the flow injects from the nozzle, three sides of the flow will face the ambient air. If the curved surface is also three-dimensional, the separation of the flow may not only occur in the radial direction. When considering the lateral flow, the wet area of the flow on the surface may also change. There is no doubt that the teapot effect is a complex three-dimensional problem.[31] In our study, the curved surface is a two-dimensional cylinder and the lateral flow is slow enough to be negligible. The flow is simplified to a fixed-width two-dimensional rectangular fluid.

For a steady two-dimensional flow of an incompressible fluid developed on a cylindrical surface, there is a balance between the centrifugal force F_c (resulting from the inertia of the fluid flow) and the centripetal force. (Note that the centrifugal force F_c does not exist physically. But the dynamics problem can be transformed into a static problem by introducing this imaginary inertial force.) The velocity contour for curved flow can be calculated based on the boundary-layer type equations,[24] as shown in Figure 1e. There is a maximum velocity at position y_m of the flow velocity contour and the flow layers can be divided into external layer and inner layer by y_m. In the external layer, the velocity in the curved flow decreases as the distance from the center of the streamline curvature to the surface increases, which induces a pressure difference acting as a centripetal force according to Bernoulli's equation. While in the inner layer, velocity contour is influenced by the boundary shear force. The capillary adhesion force F_{ca}, which is the adhesion force between the solid and liquid surface, acts as the centripetal force.

When the centrifugal force exceeds the capillary adhesion force, the inner layer of the curved flow would separate from the solid surface (the critical velocity is described by V_s). If the capillary adhesion force is strong enough, the separation would occur between flow sheets (which is called splashing with a critical velocity V_p). As mentioned above, the cohesive force F_{co}, instead of the pressure drop inside the flow, acts as the centripetal force from the view of intermolecular interaction for flow splashing behaviors.

Based on the above description, on the condition of $F_{co} > F_{ca}$, the centrifugal force, F_c, will preferentially balance with F_{ca} and the liquid will separate completely from the solid surface without splashing (shown in Figure 1c). On the condition of $F_{co} < F_{ca}$, the centrifugal force, F_c, will preferentially balance with F_{co} and the external layer will separate from inner layer. The splashing will occur (shown in Figure 1d).

The capillary adhesion force between liquid and solid surface, F_{ca}, is closely related to liquid surface tension γ. The liquid viscosity η affects the flow velocity contour and viscous force, which is essentially one kind of the intermolecular forces. Liquids with different additive molecules show different bonding energy E_b, which is closely related to the cohesive force F_{co}. Therefore, in this Section, the effect of these liquid properties on the splashing behavior, actually on the comparison of F_{co} and F_{ca}, will be discussed.

4.1 Surface tension effect: flow behaviors of water and SDS solutions

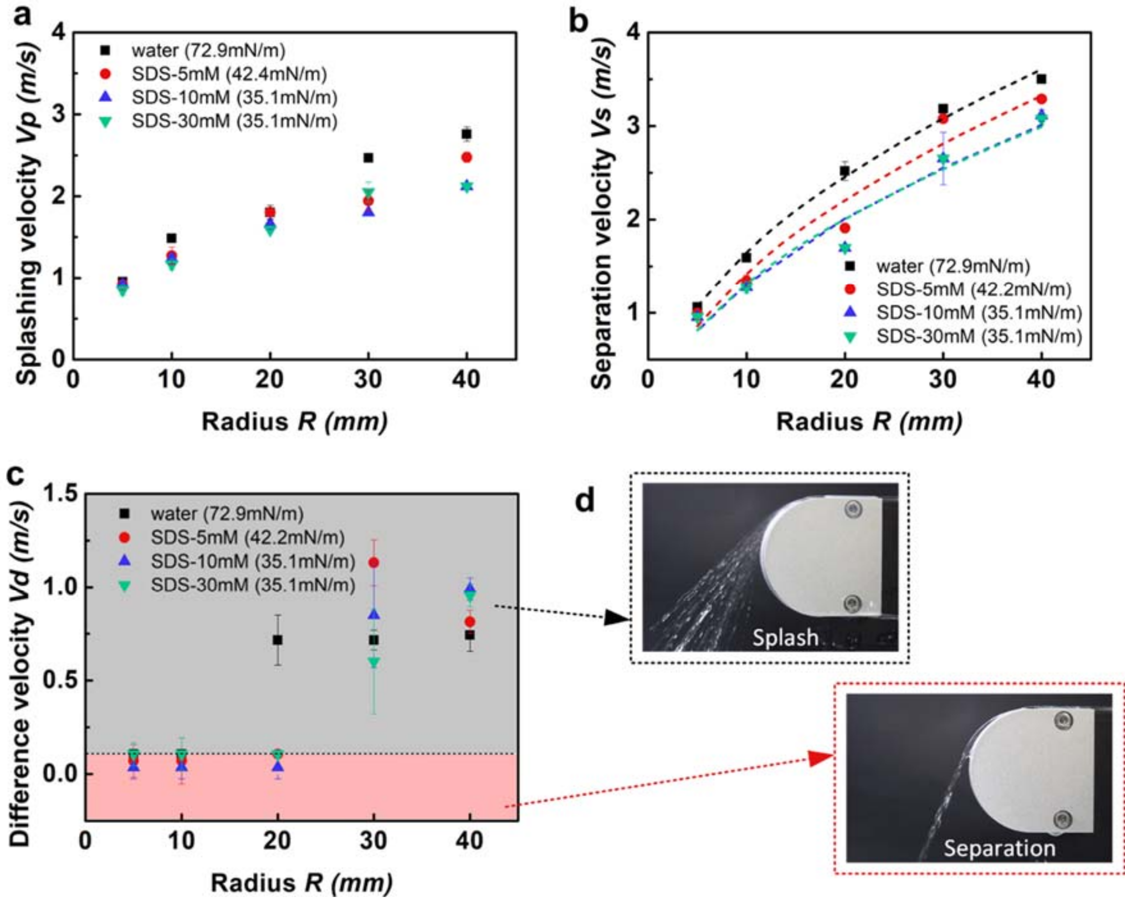

Figure 2. Flow behaviors of water and SDS solutions in teapot effect. (a-c) The evolution of V_p, V_s and V_d with aluminum plate radius, respectively. (d) Pictures of typical flow behaviors of splashing and separation.

To understand the flow splashing behaviors, three dimensionless numbers of hydrodynamics need to be introduced, which are Reynolds number $Re = \rho U a/\eta$, Weber number $We = \rho U^2 a/\gamma$ and Froude number $Fr = ga/U^2$ (with U the velocity, ρ the density, η the shear viscosity, γ the surface tension, g the gravity constant, and a typical length scale). For characteristic values in this study around $U{\sim}1m/s$, $\rho{\sim}10^3\text{kg/m}^3$, $\eta{\sim}1\text{mPa}\cdot\text{s}$, γ~70mN/m and the thickness of water jet $a{\sim}1mm$, the Re number is about 10^3, Fr number is about 10^{-2}, and We number is of order 10. Generally, small Froude number ($Fr \ll 1$) means gravity plays a negligible role. The We number is moderate and the surface tension should be sincerely considered. Actually the surface property is one of the main factors affecting the teapot effect.

As shown in Table 1, the SDS molecules will decrease the liquid surface tension and contact angle on the aluminum plate. Figure 2a and b show the evolution of V_p and V_s with the solid plate radius R, respectively. When R is less than 20 mm, the splashing velocity of water and SDS solutions are almost the same. When R is larger than 20 mm, the water splashing velocity is larger than SDS solutions as shown in Figure 2a. The separation velocity of water is larger than that of the SDS solutions as shown in Figure 2b, which indicates that V_s increases as the surface tension increases. This can be explained by the force balance between the centrifugal force F_c and the capillary adhesion force F_{ca}.[17]

The centrifugal force acted on the fluid is

$$F_c = \frac{\rho e S v^2}{R+e} \qquad (3),$$

where ρ is the density of liquids, e is the thickness of liquid layer when it flows on the plate, S is the wetted area. The maximum capillary adhesion force is

$$F_{ca} \sim \frac{\gamma S(1+cos\theta)}{e} \qquad (4)$$

where θ is the contact angle. When $F_{ca} = F_c$, the separation velocity V_s could be expressed as

$$V_s \sim \frac{1}{e}\sqrt{\frac{\gamma(R+e)(1+cos\theta)}{\rho}} \qquad (5)$$

That means the minimal velocity for liquid to separate from the solid surface (V_s) is closely related to the surface tension γ and contact angle θ.V_s is also predicted approximately proportional to $\sqrt{R}$, which shows the same tendency with Figure 2b.

Figure 2c shows that the values V_d of water and SDS solutions. A high value of V_d represents the solution is easier to splash (shown in the gray area in Figure 2d). If V_d is close to 0 (smaller than 0.15 m/s), it is considered no splashing stage, which means the liquid will separate from the plate surface as a group, as shown in the pink area in Figure 2d. Thus, V_d can be used to distinguish whether the splashing behavior happens. Figure 2c shows no splashing for small solid plate radius. It could be ascribed to the small radius induces small wetted area, which leads to a small capillary adhesion force according to Equation (4). As the solid plate radius increases, the increase of the capillary adhesion force is larger than that of the cohesive force so that the liquid jet would splash at large radius.

However, the values V_d for different liquids are very close for large solid plate radius (e.g. 40mm), as shown in Figure 2c. It could be explained that the surface tensions of SDS solutions are almost equal to water under high flow velocity. That attributes to the absorption of SDS on the new interface of liquid and air needs some time[32,33]. On this condition, the capillary adhesion force F_{ca} of water and SDS solutions are equivalent.

4.2 Viscosity effect: splashing behaviors of water and GL solutions

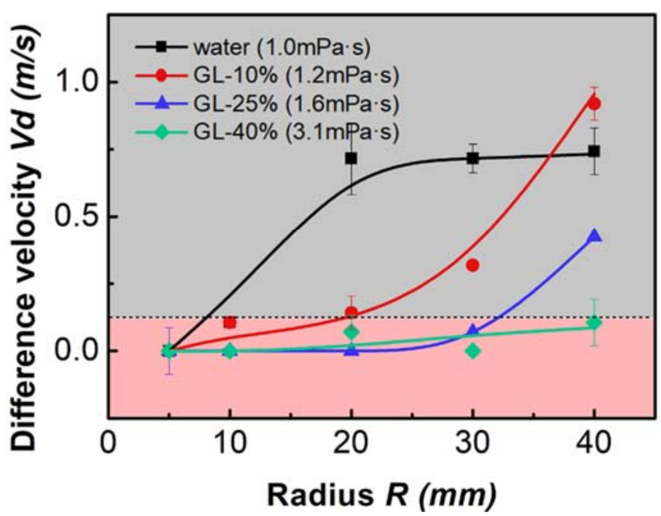

Figure 3. The evolution of V_d of different viscosity solutions as a function of aluminum plate radius.

Distilled water and GL solutions with different mass fraction were used to study the viscosity effect on the splashing behavior of teapot effect. GL has small molecular weight and GL solutions have closer surface tensions with water (shown in Table 1). As estimated in Section 3.1, a large Reynolds number ($Re{\sim}10^3$) indicates that flow is under an inertia-rule condition and the effect of viscosity is weak. However, when splashing occurs, the thickness of water jet will be much smaller (e.g. $a{\sim}0.1$mm), the *Re* number will be not so large and the liquid viscosity effect cannot be neglected. Moreover, liquid with a higher viscosity has a lower *Re* number, which means the viscosity affects more to the flow behaviors for high viscosity liquid.

Results showed that GL liquids with a higher viscosity (lower *Re* number) have a smaller V_d (shown in Figure 3), which means that they are more difficult to splash. When the GL solutions viscosity is larger than about 3 mPa·s, the splashing behavior tends to disappear and the liquid will separate from the plate surface in a single group. When the flow velocity distributions have little difference (shown in Figure S3b), a larger viscosity means a larger viscous force. Viscous force provides a resistance for the flow sheets separation process, which is closely related to the cohesive force. Therefore, a higher viscosity of GL solution induces a higher cohesive force, which makes it more difficult to splash. How viscosity affecting the cohesive force deserves further investigation with the help of molecular dynamic simulations by comparing different additive solutions of the same viscosity.

4.3 Additive effect: splashing behaviors of GL, PEG and PAM solutions

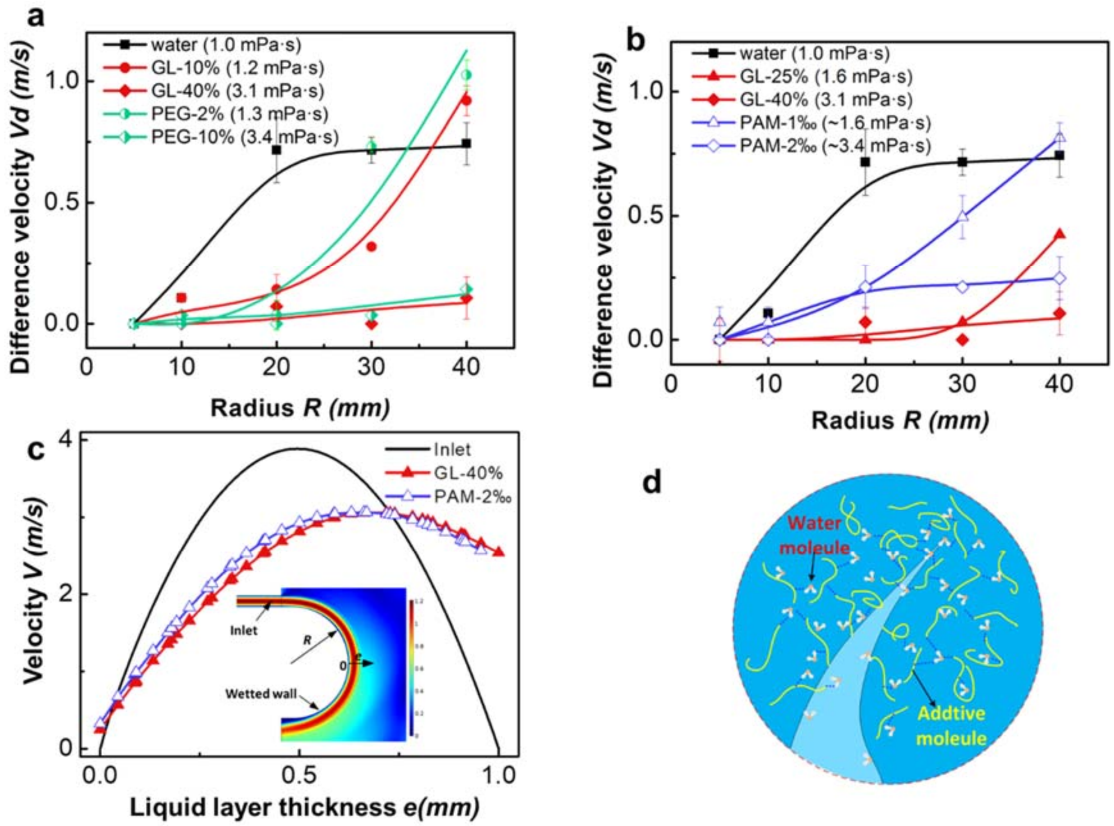

Figure 4. Molecular additives effect on the viscosity and splashing behaviors. (a)(b) The evolution of V_d with the aluminum plate radius. Water, GL and PEG solutions are compared in (a). Water, GL and PAM solutions are compared in (b). Note that the data of V_d for water and GL-40% are repeated in (a) and (b) for comparison of the liquids of the same viscosity. (c) Flow velocity contours of the inlet flow and curved flows (GL and PAM solutions). The location of the curved flow is indicated in the insert with an arrow (o-e). The insert is a typical velocity profile of the simulation result. (d) Schematic of splashing mechanism. The water molecules detach from additive molecules in the splashing area. The dashed blue lines indicate the intermolecular interactions. This figure is an enlarged view of the red circle area in Figure 1e.

PEG, PAM and GL solutions are prepared to study the additive effect on the splashing behaviors. Figure S3a (SI Section S3) shows that the GL and PEG solutions are Newtonian fluids, but the

PAM solutions are non-Newtonian fluids, of which the viscosity decreases as the shear rate increases. When the viscosity of PEG solutions is similar to the GL solution (shown in Figure S3a), the splashing behaviors for the two solutions are almost the same as shown in Figure 4a, which is consistent with the analysis in Section 3.2. However, the PAM solution is easier to splash than the GL solution as shown in Figure 4b. The viscosity of the selected PAM solution is very close to the viscosity of the selected GL solutions when the shear rate is larger than 1000 1/s (e.g. GL-25% solution and PAM-1‰ solution; GL-40% solution and PAM-2‰ solution). Figure 4a and b indicate that non-Newtonian fluids are easier to splash than Newtonian fluids, even on the condition of the same viscosity.

To reveal the difference of non-Newtonian fluids and Newtonian fluids in teapot effect, a finite element simulation model was used to calculate the velocity contour of the water flow. Figure 4c shows the velocity profiles of the inlet and curved flow of the two fluids when the plate radius is 30 mm. In the simulation, the viscosity of PAM-2‰ is expressed as (by fitting the viscosity-shear rate curve in Figure S3a)

$$\eta_{\mathrm{PAM-2‰}} = 10.9\tau^{-0.16} \quad (6),$$

where τ is the shear rate. Figure 4c represents that the velocity profile for PAM solutions is almost the same as GL solution. It means that “shear thinning” property of the PAM solution has little effect on the flow velocity profile or the splashing behavior. The bonding force between the different additive and water molecules, which is related to the cohesive force, should be considered responsible for the significantly different splashing behavior.

The bonding force is dependent on the bonding energy E_b between water and additive molecules, which could be calculated by the molecular dynamics simulation results. [34,35] The bonding energy of water and the additive molecules could be quantitatively expressed as:

$$\Delta E_{water/A} = E_{water/A} - E_A - E_{water} \qquad (7),$$

where $E_{water/A}$ is the total energy of A solution. E_A and E_{water} are the total energies of all A molecules and water molecules, respectively. Here A could represent GL, PEG or PAM. As a result of the existence of bonding force between water and additive molecules, the liquid is hold together by "additive-water-additive", and the cohesive energy of the liquid increases. When splashing occurs, the additive molecules need to separate from water molecules so that the stream layer detaches from the liquid jet as sketched in Figure 4d.

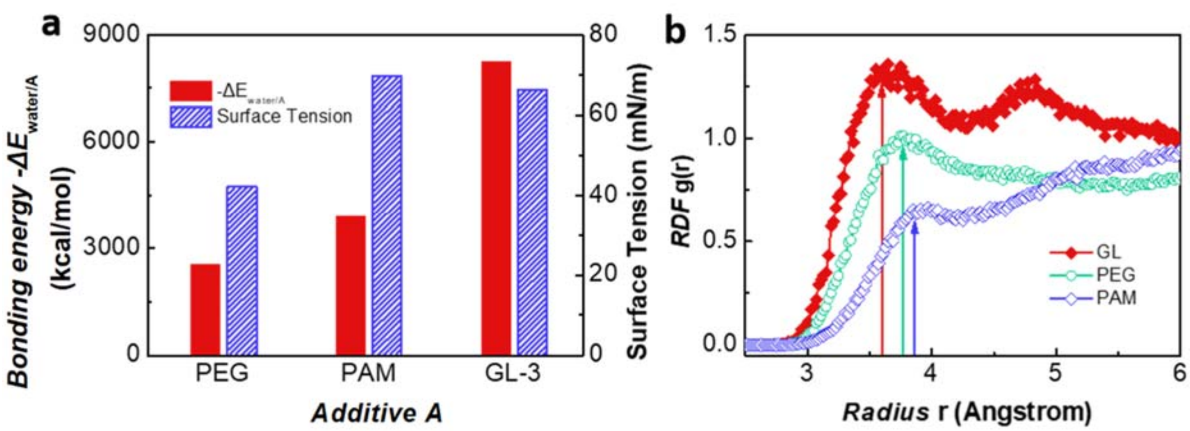

Figure 5. Molecular dynamics simulation results of GL, PEG and PAM solutions. (a) Bonding energy and surface tension of different additive molecule liquids. (b) Radial distribution function of GL, PEG and PAM solutions.

Based on the molecular dynamics simulation, the bonding energy of additive molecules with water is calculated. Figure S4 (SI Section S4) shows the molecular structures and charge differences of water, GL, PEG and PAM molecules. The different value and location of charge contribute different bonding energy of water and GL, PEG and PAM. The hydrogen bond between water and other molecules mainly depends on the charge difference of Oxygen atoms and

Hydrogen atoms. Figure 5a shows the bonding energy and surface tension for different additive solutions. The surface tensions of PAM and GL solutions are almost the same, but the bonding energy of PAM solution is much less than GL solution. Therefore, the PAM solutions are easier to satisfy the condition of $F_{co} < F_{ca}$ and are easier to splash, as shown in Figure 4b. Although the surface tension of PEG solution is much less than GL solution, the bonding energy is also much less than GL solution. Therefore, the PEG solutions show similar splashing behaviors with GL solutions, as show in Figure 4a.

In statistical mechanics, the radical distribution function (RDF) describes the density of a system of particles varies as a function of distance from the reference particles. The RDF could be used to compare the number density of water molecules near different additive molecules. Carbon atoms are considered the center atoms of additive molecules and Oxygen atoms are the center atoms of water. The RDF of Carbon atoms and Oxygen atoms in the system is shown in Figure 5b. The position of the maximum usually explains the hydrogen-bonding length or the location of water molecules near the additive. The peak value expresses the relative strength of hydrogen bond or the density of water molecules. [36,37] Figure 5b shows that the number density of water molecules near GL molecules is much larger than the other two kinds of molecules. While the density of water molecules near PAM molecule is the smallest and the distance of water to the PAM molecule is the longest. When the total numbers of Carbon atoms are the same, the lower water number density and longer distance of water to additive molecules are accompanied with lower cohesive force such as PAM (shown in Figure 5b), which will make the PAM solutions easier to splash. While the higher water density and smaller distance of water to molecules are accompanied with higher cohesive force such as GL and PEG (shown in Figure 5b), which will induce the GL and PEG solutions easier to separate completely from solid surface instead of splashing. Based on the above molecular dynamic simulation results, we conclude that the density and location of water molecules are the main mechanisms attributing to the PAM solutions easy to splash.

4. CONCLUSIONS

In this study, liquid surface tension, viscosity and additive effects on the splashing behaviors in teapot effect have been studied. Experimental results showed that the splashing behaviors were not only dependent on the liquid surface tension and viscosity but also on the additive molecules. Based on the molecular dynamics simulations results, the bonding energy for different kinds of additives may influence the cohesive force of the liquids. A higher cohesive force is accompanied with a higher density of the water molecules near additive molecules. The solution is more strongly held together and tends to flow in a single stream. The relative magnitude of the cohesive force and capillary adhesion force significantly affects the splashing behaviors. When the cohesive force F_{co} is larger than capillary adhesion force F_{ca}, there is always no splashing even when the jet velocity is high. Otherwise, the liquid would splash from the liquid jet. These results present a new insight into the splashing mechanism in teapot effect.

ASSOCIATED CONTENT

Supporting Information

Flow evolution at different velocities and radius; Simulation method; Viscosity and simulation velocity contours; Charge of additive molecules (PDF)

AUTHOR INFORMATION

Corresponding Author

*E-mail: tianyu@tsinghua.edu.cn. Tel: +86-10-62782981.

Author Contributions

The manuscript was written through contributions of all authors. All authors have given approval to the final version of the manuscript.

Notes

The authors declare no competing financial interest.

ACKNOWLEDGMENTS

This work is sponsored by the Natural Science Foundation of China with Grant No. 51425502. We sincerely thank Dr. Hongyu Lu for the help of conducting experiments. We sincerely thank Dr. Chuke Ouyang and Dr. Pengpeng Bai for helping on the pictures of teapot effect.

REFERENCES

(1) Lee, H.; Han, S.; Lee, H.; Jeon, J.; Lee, C.; Kim, Y. B.; Song, S. H.; Choi, H. R., Design Optimization, Modeling, and Control of Unmanned Aerial Vehicle Lifted by Coandă Effect. *IEEE/ASME T. Mech.* **2017**, *22*, 1327-1336.

(2) Dickerson, A. K.; Shankles, P. G.; Hu, D. L., Raindrops Push and Splash Flying Insects. *Phys. Fluids* **2014**, *26*, 027104.

(3) Pitton, G.; Quaini, A.; Rozza, G., Computational Reduction Strategies for the Detection of Steady Bifurcations in Incompressible Fluid-Dynamics: Applications to Coanda Effect in Cardiology. *J Comput. Phys.* **2017**, *344*, 534-557.

(4) Gallacher, J. R.; Ripa, B.; Butler, B. W.; Fletcher, T. H., Lab-Scale Observations of Flame Attachment On Slopes with Implications for Firefighter Safety Zones. *Fire Saf. J.* **2018**, *96*, 93-104.

(5) Borruto, A.; Crivellone, G.; Marani, F., Influence of Surface Wettability On Friction and Wear Tests. *Wear* **1998**, *222*, 57-65.

(6) Neurouth, A.; Changenet, C.; Ville, F.; Octrue, M.; Tinguy, E., Experimental Investigations to Use Splash Lubrication for High-Speed Gears. *J. Tribol.* **2017**, *139*, 061104.

(7) Reiner, M., The Teapot Effect…a Problem. *Phys Today* **1956**, *9*, 16.

(8) Dong, Z.; Wu, L.; Wang, J.; Ma, J.; Jiang, L., Superwettability Controlled Overflow. *Adv Mater* **2015**, *27*, 1745-1750.

(9) Keller, J. B., Teapot Effect. *J. Appl. Phys.* **1957**, *28*, 859-864.

(10) Guyon, E.; Hulin, J.; Petit, L.; Mitescu, C. D., *Physical Hydrodynamics*; Oxford University Press: New York, 2015.

(11) Vanden Broeck, J. M.; Keller, J. B., Pouring Flows. *Phys. Fluids* **1986**, *29*, 3958-3961.

(12) Vanden Broeck, J. M.; Keller, J. B., Pouring Flows with Separation. *Phys. Fluids A* **1989**, *1*, 156-158.

(13) Coanda, H., Lifting Device Coanda Effect. *US Patent* **1936**.

(14) Newman, B. G., The Deflection of Plane Jets by Adjacent Boundaries—Coanda Effect. *Boundary layer and flow control* **1961**, *1*, 232-264.

(15) Skotnicka-Siepsiak, A., Hysteresis of the Coanda Effect. *J. Fluids Eng.* **2018**, *140*, 011202.

(16) Israelachvili, J. N., *Intermolecular and Surface Forces*; Academic Press: New York, 2011.

(17) Duez, C.; Ybert, C.; Clanet, C.; Bocquet, L., Wetting Controls Separation of Inertial Flows From Solid Surfaces. *Phys. Rev. Lett.* **2010**, *104*, 84503.

(18) Bouwhuis, W.; Snoeijer, J. H., The Effect of Surface Wettability On Inertial Pouring Flows. *arXiv preprint arXiv:1507.05931* **2015**.

(19) Bouwhuis, W., *Dynamics of Deforming Drops*; Universiteit Twente, 2015.

(20) Kibar, A. Experimental and Numerical Investigations of the Impingement of an Oblique Liquid Jet onto a Superhydrophobic Surface: Energy Transformation. *Fluid Dyn. Res.* **2016**, *48(1)*, 015501.

(21) Kibar, A., Experimental and Numerical Investigation of Liquid Jet Impingement On Superhydrophobic and Hydrophobic Convex Surfaces. *Fluid Dyn. Res.* **2017**, *49(1)*, 15502.

(22) Taylor, G.; Howarth, L. *The Dynamics of Thin Sheets of Fluid. I. Water Bells*, *Proc. R. Soc. Lond. A* **1959**, 289-295.

(23) Clanet, C., Waterbells and Liquid Sheets. *Annu. Rev. Fluid Mech.* **2007**, *39*, 469-496.

(24) Isshiki, H.; Yoon, B.; Yum, D., Separation of Sheet Flow On the Surface of a Circular Cylinder. *Phys. Fluids* **2009**, *21*, 082104.

(25) Dumitrache, A.; Frunzulica, F.; Ionescu, T. C., Mathematical Modelling and Numerical Investigations On the Coanda Effect. *Nonlinearity, Bifurcation and Chaos-Theory and Applications*, InTech: 2012.

(26) Feng, Y.; Song, Y.; Chen, F., Numerical Simulation of Circulation Control Turbine Cascade with Coanda Jet and Counter-Flow Blowing at High Mach Numbers. *Aeronaut. J.* **2017**, *121*, 1239-1260.

(27) Olsson, E.; Kreiss, G., A Conservative Level Set Method for Two Phase Flow. *J. Comput. Phys.* **2005**, *210*, 225-246.

(28) Lafaurie, B.; Nardone, C.; Scardovelli, R.; Zaleski, S.; Zanetti, G., Modelling Merging and Fragmentation in Multiphase Flows with Surfer. *J. Comput. Phys.* **1994**, *113*, 134-147.

(29) Choi, Y. J.; Choi, J. H.; Choi, K. M.; Kang, J. K., Covalent Organic Frameworks for Extremely High Reversible CO_2 Uptake Capacity: A Theoretical Approach. *J. Materials Chem.* **2011**, *21 (4)*, 1073-1078.

(30) Wang, C. X.; Zu Chen, W.; Tran, V.; Douillard, R., Analysis of Interfacial Water Structure and Dynamics in α-Maltose Solution by Molecular Dynamics Simulation. *Chem. Phys. Lett.* **1996**, *251*, 268-274.

(31) Gregory-Smith, D. G.; Gilchrist, A. R., The Compressible Coanda Wall Jet—An Experimental Study of Jet Structure and Breakaway. *Intl. J. Heat and Fluid Flow* **1987**, *8 (2)*, 156-164.

(32) Bonfillon, A.; Sicoli, F.; Langevin, D., Dynamic Surface Tension of Ionic Surfactant Solutions. *J. Colloid Interface Sci.* **1994**, *168*, 497-504.

(33) Song, M.; Ju, J.; Luo, S.; Han, Y.; Dong, Z.; Wang, Y.; Gu, Z.; Zhang, L.; Hao, R.; Jiang, L., Controlling Liquid Splash On Superhydrophobic Surfaces by a Vesicle Surfactant. *Sci. Adv.* **2017**, *3*, e1602188.

(34) Bondesson, L.; Mikkelsen, K. V.; Luo, Y.; Garberg, P.; Ågren, H., Density Functional Theory Calculations of Hydrogen Bonding Energies of Drug Molecules. *J. Mol. Struct.: THEOCHEM* **2006**, *776*, 61-68.

(35) Zhang, M.; Chen, L.; Yang, H.; Ma, J., Theoretical Study of Acetic Acid Association Based On Hydrogen Bonding Mechanism. *J. Phys. Chem. A* **2017**, *121*, 4560-4568.

(36) Sagarik, K.; Rode, B. M., Intermolecular Potential for Benzoic Acid – Water Based On the Test-Particle Model and Statistical Mechanical Simulations of Benzoic Acid in Aqueous Solutions. *Chem. Phys.* **2000**, *260*, 159-182.

(37) Meng, S.; Li, W.; Yin, X.; Xie, J., A Comprehensive Theoretical Study of the Hydrogen Bonding Interactions and Microscopic Solvation Structures of a Pyridyl-Urea-Based Hydrogelator in Aqueous Solution. *Comput. Theor. Chem.* **2013**, *1006*, 76-84.

TOC Graphic

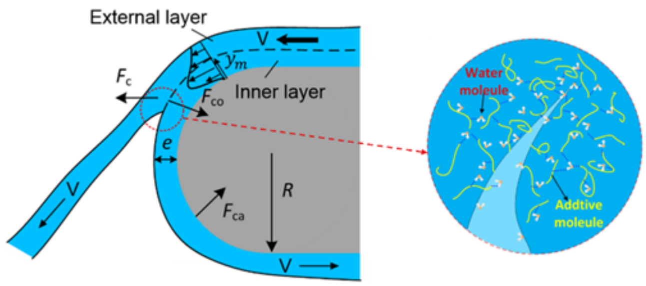
External layer
V
y_m
F_c
F_{co}
Inner layer
e
R
F_{ca}
V
V
Water
moleule
Addtive
moleule

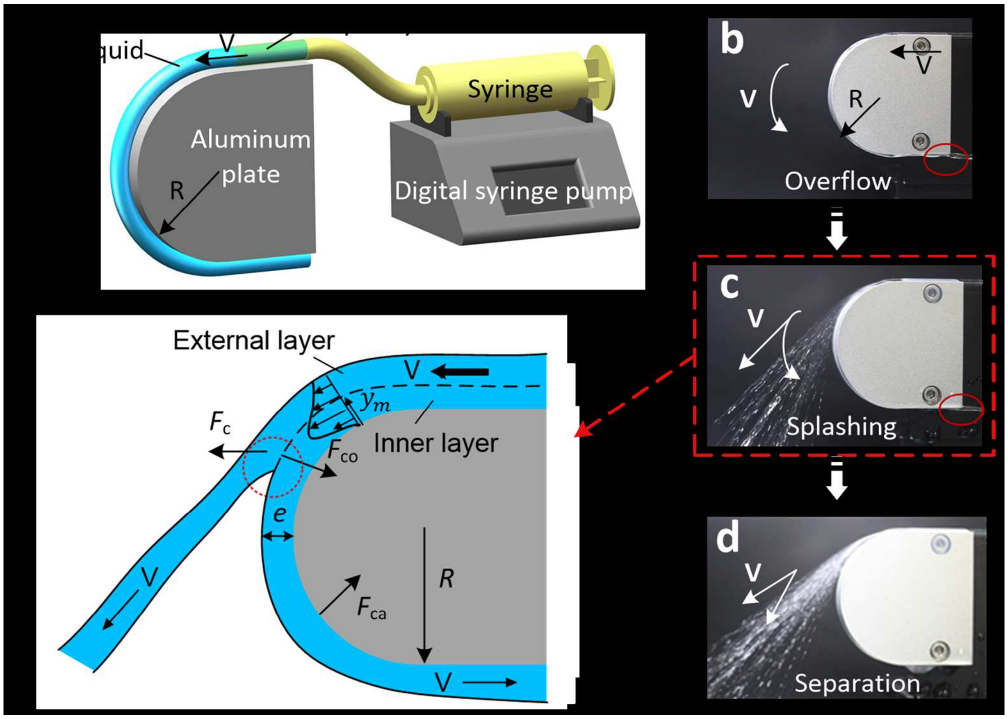

Figure 1. Schematic of the experiment. (a) Schematic of the test system. The flow was drove by a digital syringe pump (RISTRON, RSP02-B, Zhejiang, China) and the nozzle was a capillary tube with an inner diameter of 1 mm. The radius of aluminum plates, R, ranged from 5 mm to 40 mm. (b)(c)(d) Flow behaviors evolve with the increase of average outflow velocity. For water solution, the flow behaviors will present overflow (b), splashing (c) and separation (d) successively. (e) Schematic of splashing behavior. F_c, F_{ca} and F_{co} represent the centrifugal force, capillary adhesion force and cohesive force between the stream layers, respectively.

262x186mm (150 x 150 DPI)

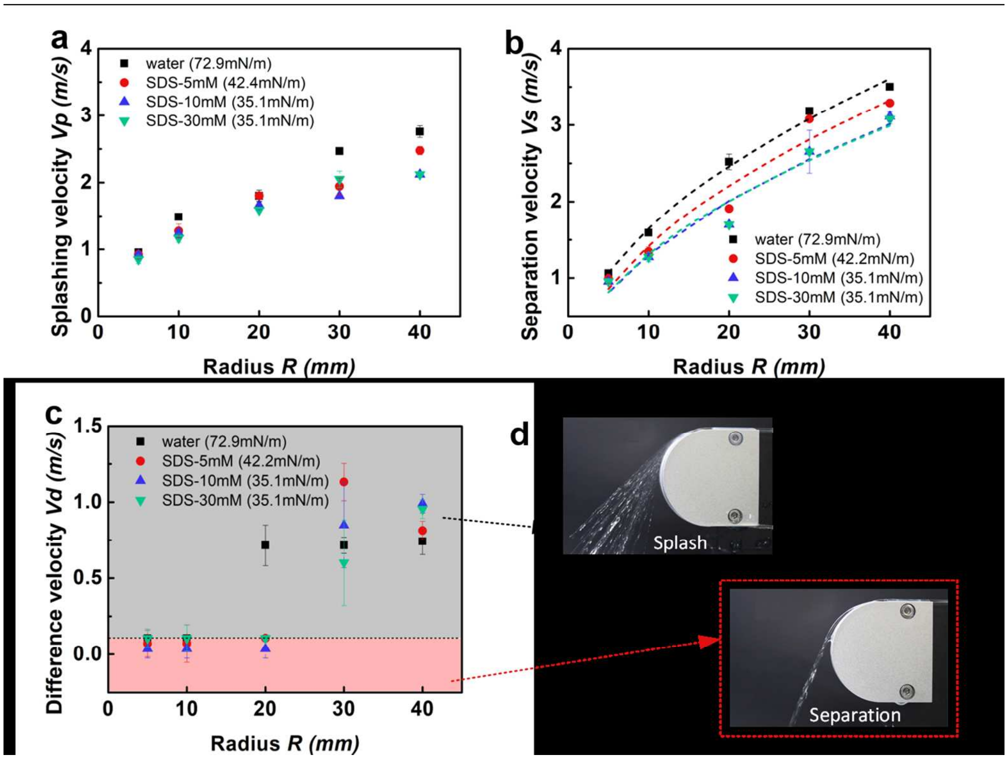

Figure 2. Flow behaviors of water and SDS solutions in teapot effect. (a-c) The evolution of V_p, V_s and V_d with aluminum plate radius, respectively. (d) Pictures of typical flow behaviors of splashing and separation.

250x188mm (150 x 150 DPI)

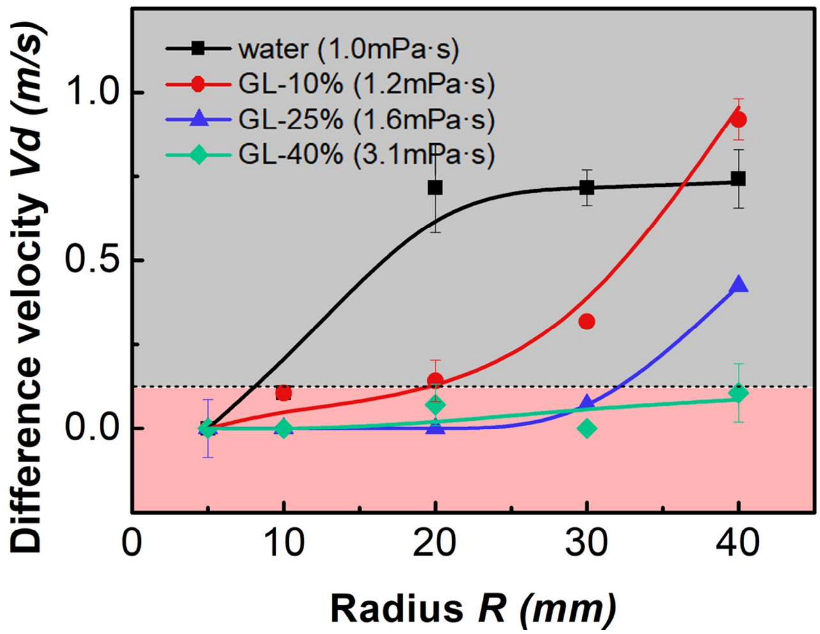

Figure 3. The evolution of V_d of different viscosity solutions as a function of aluminum plate radius.

251x176mm (150 x 150 DPI)

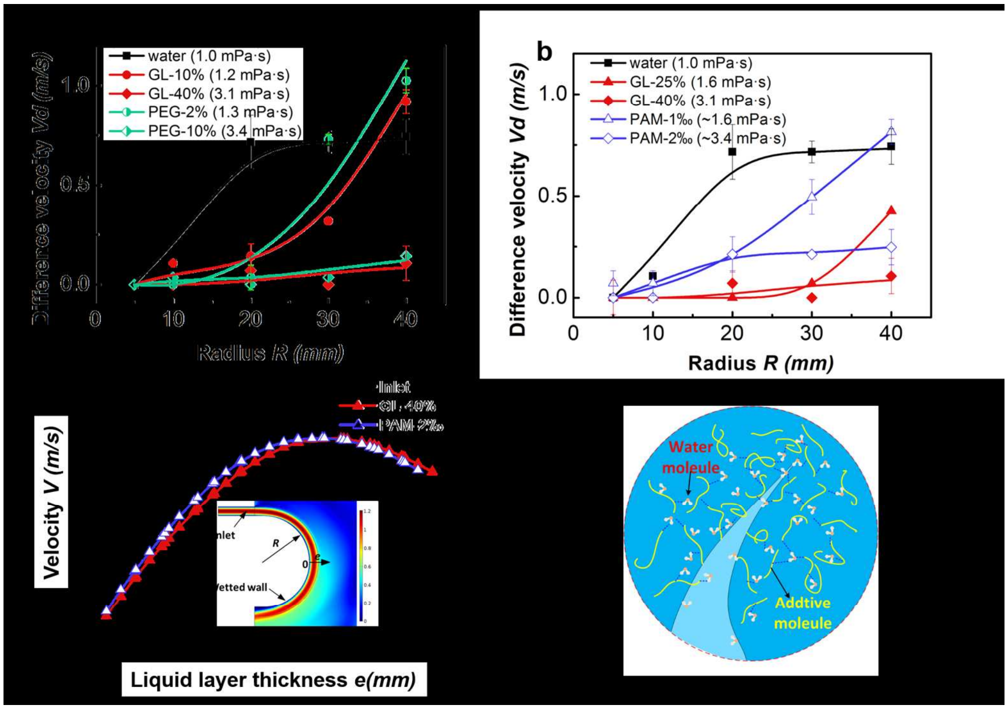

Figure 4. Molecular additives effect on the viscosity and splashing behaviors. (a)(b) The evolution of V_d with the aluminum plate radius. Water, GL and PEG solutions are compared in (a). Water, GL and PAM solutions are compared in (b). Note that the data of V_d for water and GL-40% are repeated in (a) and (b) for comparison of the liquids of the same viscosity. (c) Flow velocity contours of the inlet flow and curved flows (GL and PAM solutions). The location of the curved flow is indicated in the insert with an arrow (o-e). The insert is a typical velocity profile of the simulation result. (d) Schematic of splashing mechanism. The water molecules detach from additive molecules in the splashing area. The dashed blue lines indicate the intermolecular interactions. This figure is an enlarged view of the red circle area in Figure 1e.

306x214mm (150 x 150 DPI)

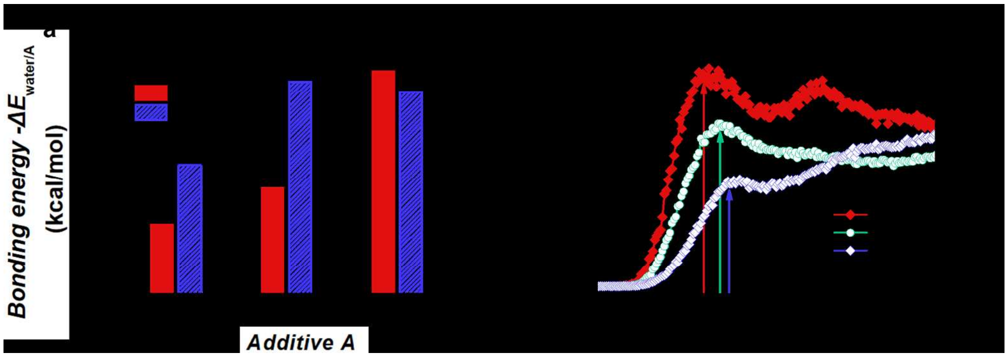

Figure 5. Molecular dynamics simulation results of GL, PEG and PAM solutions. (a) Bonding energy and surface tension of different additive molecule liquids. (b) Radial distribution function of GL, PEG and PAM solutions.

394x137mm (150 x 150 DPI)